J|A|C|S
COMMUNICATIONS

Published on Web 09/05/2002

High-Resolution NMR Spectroscopy of Quadrupolar Nuclei in Solids: Satellite-Transition MAS with Self-Compensation for Magic-Angle Misset

Sharon E. Ashbrook and Stephen Wimperis*

School of Chemistry, University of Exeter, Exeter EX4 4QD, United Kingdom

Received March 14, 2002

Several methods are available for obtaining high-resolution NMR spectra of half-integer spin quadrupolar nuclei, such as ^{11}B, ^{23}Na ($I = {}^3/_2$) and ^{17}O, ^{27}Al ($I = {}^5/_2$), in powdered solids.[1−3] Satellite-transition magic-angle spinning (STMAS)[3] uses only conventional magic-angle spinning (MAS) hardware and, it has been claimed,[4] improves significantly upon the signal-to-noise ratio obtained with the widely adopted multiple-quantum MAS (MQMAS) experiment.[2] The STMAS technique, however, requires that the sample rotation axis be set to the magic angle ($\cos^{-1}(1/\sqrt{3}) = 54.736°$) with respect to the magnetic field B_0 with an accuracy of better than $\pm 0.004°$,[3,4] and this stringent requirement has severely limited the use of the method. Here, we propose a novel version of STMAS that self-compensates for magic-angle missets of up to $\pm 1.0°$ and yet retains a sensitivity similar to that of MQMAS.

Under MAS, central transition ($m_I = -{}^1/_2 \leftrightarrow m_I = +{}^1/_2$) NMR spectra of half-integer spin quadrupolar nuclei remain broadened by a second-order quadrupolar interaction.[5] In a reference frame rotating at the Larmor frequency ν_0, the frequency of an observable $m_I = \pm(q - 1) \leftrightarrow m_I = \pm q$ transition (with $q = {}^1/_2, {}^3/_2, ..., I$) can be written for a rapidly spinning sample as the sum of two terms arising from the first- and second-order quadrupolar interactions, respectively:

$$\nu^{(1)}_{\pm(q-1)\leftrightarrow\pm q} = \pm(2q-1)\nu_Q^{PAS} d^2_{0,0}(\chi) d^2_{0,0}(\beta) \quad (1a)$$

$$\nu^{(2)}_{\pm(q-1)\leftrightarrow\pm q} = \frac{(\nu_Q^{PAS})^2}{\nu_0}\{A^0(I,q) + A^2(I,q) d^2_{0,0}(\chi) d^2_{0,0}(\beta) + A^4(I,q) d^4_{0,0}(\chi) d^4_{0,0}(\beta)\} \quad (1b)$$

Here, χ is the angle between the spinning axis and B_0, β is the orientation of the quadrupole tensor (for simplicity, axial symmetry is assumed) with respect to the spinning axis, the coefficients $A^l(I, q)$ are derived from perturbation theory,[2,3,6] and the quadrupole parameter, ν_Q^{PAS}, is given by $3e^2qQ/\{4I(2I-1)h\}$. Spinning at the magic angle, the rank $l = 2$ rotation matrix element, $d^2_{0,0}(\chi = 54.736°)$, is zero, and the first-order quadrupolar splitting is removed from all transitions in which it occurs. However, the anisotropic second-order shift survives because the $l = 4$ element, $d^4_{0,0}(\chi = 54.736°)$, is nonzero. In a powder, there is a spherical distribution of β angles, and the result is a MAS spectrum with a central transition (CT) that has a rank $l = 4$ broadening proportional to $A^4(I, {}^1/_2)(\nu_Q^{PAS})^2/\nu_0$ and an isotropic quadrupolar shift equal to $A^0(I, {}^1/_2)(\nu_Q^{PAS})^2/\nu_0$.

The pulse sequence for a shifted-echo[7] two-dimensional STMAS experiment[4] is shown in Figure 1a. This technique removes the first- and second-order quadrupolar broadening (i) by using MAS to suppress the first-order splitting and the rank $l = 2$ component of the second-order interaction and (ii) by correlating the two $q = {}^3/_2$ satellite transitions (usually, although $q = {}^5/_2$, ${}^7/_2$, and ${}^9/_2$ transitions have also been used[4]) in the t_1 period with the $q = {}^1/_2$ central transition in the t_2 period such that an echo forms when $t_2/t_1 = A^4(I, {}^3/_2)/A^4(I, {}^1/_2)$, refocusing the $l = 4$ second-order broadening. As desired, the method retains resolution due to isotropic (rank $l = 0$) shifts. Figure 2a shows the ^{87}Rb ($I = {}^3/_2$) STMAS spectrum of $RbNO_3$. The three crystallographically inequivalent Rb sites appear as three "ridge" line shapes (two lie very close together) with gradients equal to $A^4({}^3/_2, {}^3/_2)/A^4({}^3/_2, {}^1/_2) = -{}^8/_9$. In addition to these desired ST → CT ridges, an uninformative "diagonal" peak also appears along a gradient of +1

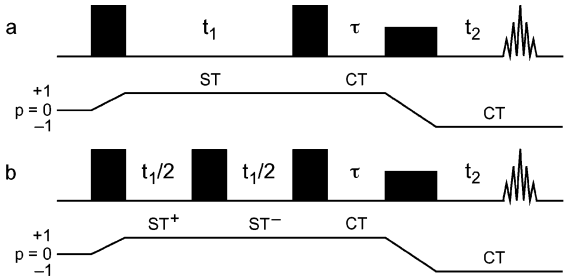

Figure 1. Pulse sequences and coherence pathways for (a) STMAS and (b) STMAS with self-compensation for magic-angle misset (SCAM). In (b), a 100-step phase cycle was used: first pulse, 0°; second pulse, 0°, 72°, 144°, 216°, 288°; third pulse, 5(0°), 5(72°), 5(144°), 5(216°), 5(288°); fourth pulse, 25(0°), 25(90°), 25(180°), 25(270°); receiver, 25(0°), 25(180°).

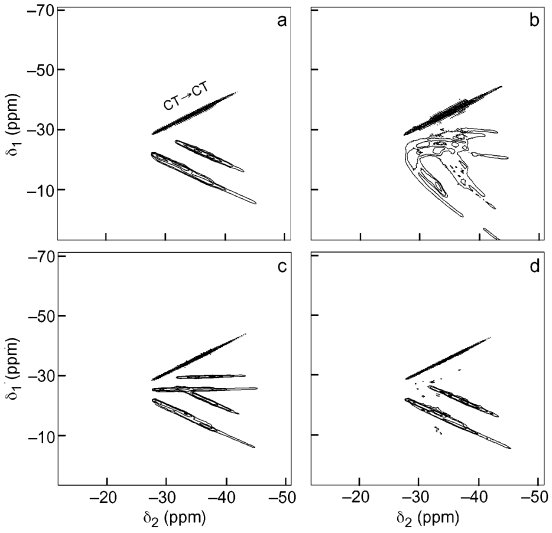

Figure 2. ^{87}Rb ($\nu_0 = 130.9$ MHz) NMR spectra of $RbNO_3$. (a) STMAS spectrum at the magic angle. The three pulse durations were 1.7 μs, 1.5 μs ($\nu_1 = |\gamma B_1| \approx 150$ kHz), and, for the final reduced-power pulse, 30 μs. (b) STMAS spectrum with the spinning angle misset by ∼0.07°. (c) SCAM-STMAS spectrum at the magic angle. (d) SCAM-STMAS spectrum with the spinning angle misset by ∼0.07°. The additional pulse durations of (c) 1.0 μs and (d) 2.0 μs were found by experimental optimization. The MAS rate, ν_R, was 20 kHz.

* To whom correspondence should be addressed. Fax: +44-1392-263434. E-mail: s.wimperis@exeter.ac.uk.

10.1021/ja0203869 CCC: $22.00

due to CT → CT coherence transfer. A high-resolution or "isotropic" spectrum can be obtained by projecting the two-dimensional spectrum onto an axis orthogonal to the $A^4(^3/_2, {}^3/_2)/A^4(^3/_2, {}^1/_2)$ gradient, as shown in Figure 3a.

The STMAS experiment requires that the spinning angle χ be set to the magic angle with high accuracy.[3,4] If χ deviates from this, then the first-order quadrupolar splitting is reintroduced. For example, the two $q = {}^3/_2$ satellites, $m_I = \pm{}^1/_2 \leftrightarrow m_I = \pm{}^3/_2$, are split by $4\nu_Q^{PAS} d^2_{0,0}(\chi) d^2_{0,0}(\beta)$, and, because a typical value of ν_Q^{PAS} is perhaps 250 kHz, the angle χ must not deviate from 54.736° by more than about ±0.004° if the splitting is not to exceed 100 Hz. In contrast, the second-order quadrupolar shifts of the central and satellite transitions are unaffected by a small deviation of χ from the magic angle. For example, if $\nu_Q^{PAS} = 250$ kHz and $\nu_0 = 100$ MHz, then $(\nu_Q^{PAS})^2/\nu_0$ is only 625 Hz, and even a ±1.0° deviation of χ changes the second-order shifts by only a few tens of Hz. Figure 2b shows the ^{87}Rb STMAS spectrum of $RbNO_3$ recorded with the angle χ misset by an amount estimated to be 0.07°. A first-order splitting has been reintroduced into the satellite-transition dimension (δ_1), and the resolution has been spoiled.

The pulse sequence for a version of STMAS that is self-compensated for angle misset (SCAM) is shown in Figure 1b. As in Figure 1a, this is a shifted-echo experiment and yields absorptive line shapes. The novel feature of the new experiment is a pulse in the middle of the t_1 period that transfers coherence between the two $q = {}^3/_2$ satellite transitions. The $m_I = +{}^1/_2 \leftrightarrow m_I = +{}^3/_2$ and $m_I = -{}^1/_2 \leftrightarrow m_I = -{}^3/_2$ transitions (ST^+ and ST^-) have first-order quadrupolar frequencies that are equal in magnitude but opposite in sign (see eq 1a); hence, by inducing $ST^{\pm} \rightarrow ST^{\mp}$ transfer, the unwanted first-order splitting is refocused. Crucially, the new pulse is phase-cycled so as to maintain the sign of the coherence order, p, and avoid premature refocusing of the second-order shift.

Figure 2c shows the ^{87}Rb SCAM-STMAS spectrum of $RbNO_3$ recorded with the spinning angle χ set accurately to the magic angle as in Figure 2a. The spectrum is similar to that in Figure 2a, except that additional ridges appear midway between the CT → CT → CT diagonal peak and the desired $ST^{\pm} \rightarrow ST^{\mp} \rightarrow$ CT and $ST^{\pm} \rightarrow ST^{\pm} \rightarrow$ CT ridges due to unwanted CT → $ST^{\pm}$ → CT and $ST^{\pm} \rightarrow$ CT → CT transfer. Figure 2d shows the ^{87}Rb SCAM-STMAS spectrum when χ is misset by ~0.07° as in Figure 2b. The unwanted CT → $ST^{\pm}$ → CT and $ST^{\pm} \rightarrow$ CT → CT ridges are now split by the residual first-order quadrupolar interaction in δ_1 and are barely visible at the contour levels used. Similarly, the $ST^{\pm} \rightarrow ST^{\pm} \rightarrow$ CT components of the desired ridges are now split and not visible. However, three narrow ridge line shapes with gradients of $-{}^8/_9$ remain prominent, arising from $ST^{\pm} \rightarrow ST^{\mp} \rightarrow$ CT pathways that refocus the first-order splitting.

The isotropic projection of a ^{87}Rb SCAM-STMAS spectrum, shown in Figure 3b, clearly reveals the three Rb sites in $RbNO_3$ but also shows reduced sensitivity as compared with STMAS performed with χ set accurately (Figure 3a). However, the sensitivity is approximately the same as that in the isotropic ^{87}Rb MQMAS projection (also performed with χ misset by ~0.07°) shown in Figure 3c. Results broadly similar to these have also been obtained on $RbNO_3$ at a lower MAS rate (10 kHz) and on Rb_2SO_4 and, using ^{27}Al ($I = {}^5/_2$) NMR, on Al(acac)$_3$ and andalusite, Al_2SiO_5.

Figure 4a shows the ^{27}Al "split-t_1"[4] STMAS ($q = {}^3/_2$) spectrum of kyanite, Al_2SiO_5, recorded with the spinning angle χ set as accurately as possible using our normal procedure.[4] There are four Al sites in kyanite, two of which have large ν_Q^{PAS} values of about 750 kHz. These two long ridge line shapes at $\delta_1 \approx 25$ ppm are not resolved in this spectrum, however, and have a distinctive "hairpin" appearance arising from residual first-order (or, possibly, third-order) splittings in δ_1 (χ would need to be misset by less than ±0.001° for the first-order splitting to be less than 100 Hz). In contrast, all four ridge line shapes are resolved in the split-t_1 SCAM-STMAS spectrum in Figure 4b, recorded with χ misset by ~0.09°; the two long ridges are now very narrow in δ_1 and precisely parallel to δ_2. This increased resolution is confirmed in the isotropic projections in Figure 4c and d.

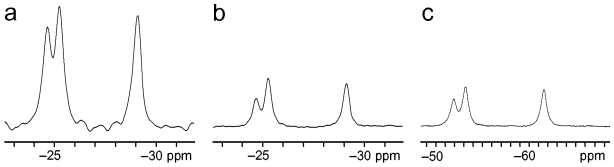

Figure 3. Absolute-intensity ^{87}Rb isotropic projections of (a) on-angle STMAS, (b) off-angle SCAM-STMAS, and (c) off-angle MQMAS (split-t_1 shifted-echo, $\nu_1 \approx 150$ kHz, $\nu_R = 20$ kHz) NMR spectra of $RbNO_3$. In (b), an experimentally optimized composite pulse, $(1.8\ \mu s)_x(1.75\ \mu s)_{-x}$, was used in place of the simple SCAM pulse to enhance the sensitivity by ~20%. In (c), an experimentally optimized fast-amplitude-modulation (FAM) conversion pulse,[8] $\{(0.8\ \mu s)_x - \tau - (0.8\ \mu s)_{-x} - \tau - \}_3$ with $\tau = 0.8\ \mu s$, was used to enhance the MQMAS sensitivity by ~80%. Each experiment was performed in 120 min with a maximum t_1 period of 24 ms.

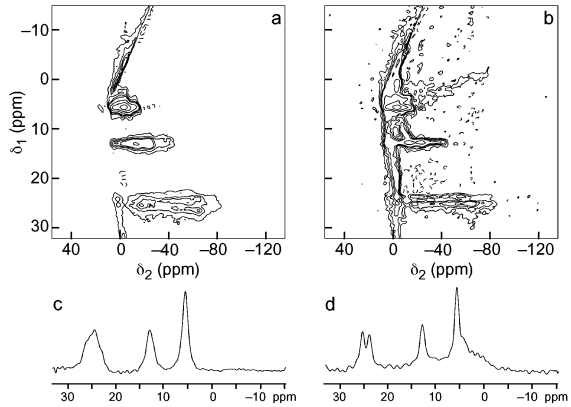

Figure 4. ^{27}Al ($\nu_0 = 104.3$ MHz) NMR spectra of Al_2SiO_5 ($\nu_1 \approx 100$ kHz, $\nu_R = 30$ kHz). (a) Split-t_1 STMAS ($q = {}^3/_2$) spectrum with the spinning angle set as accurately as possible using our normal procedure. (b) Split-t_1 SCAM-STMAS ($q = {}^3/_2$) spectrum with the angle misset by ~0.09°. (c) and (d) Normalized-intensity isotropic projections of (a) and (b).

In summary, the SCAM-STMAS NMR experiment yields superior isotropic resolution without accurate adjustment of the spinning angle (indeed, χ must be misset if the unwanted ridges in Figure 2c are to be avoided) and appears to have a sensitivity that is comparable with MQMAS. Many SCAM experiments similar to that in Figure 1b can be devised, including ones that utilize multiple-quantum satellite transitions.

Acknowledgment. We thank Professor M. H. Levitt (Southampton, U.K.) for suggesting this line of investigation to us and EPSRC for support (grant GR/N07622).

References

(1) (a) Samoson, A.; Lippmaa, E.; Pines, A. *Mol. Phys.* **1988**, *65*, 1013. (b) Llor, A.; Virlet, J. *Chem. Phys. Lett.* **1988**, *152*, 248.
(2) Frydman, L.; Harwood, J. S. *J. Am. Chem. Soc.* **1995**, *117*, 5367.
(3) (a) Gan, Z. *J. Am. Chem. Soc.* **2000**, *122*, 3242. (b) Gan, Z. *J. Chem. Phys.* **2001**, *114*, 10845.
(4) (a) Pike, K. J.; Ashbrook, S. E.; Wimperis, S. *Chem. Phys. Lett.* **2001**, *345*, 400. (b) Ashbrook, S. E.; Wimperis, S. *J. Magn. Reson.* **2002**, *156*, 269.
(5) Ganapathy, S.; Schramm, S.; Oldfield, E. *J. Chem. Phys.* **1982**, *77*, 4360.
(6) Amoureux, J. P. *Solid State Nucl. Magn. Reson.* **1993**, *2*, 83.
(7) Grandinetti, P. J.; Baltisberger, J. H.; Llor, A.; Lee, Y. K.; Werner, U.; Eastman, M. A.; Pines, A. *J. Magn. Reson., Ser. A* **1993**, *103*, 72.
(8) Madhu, P. K.; Goldburt, A.; Frydman, L.; Vega, S. *Chem. Phys. Lett.* **1999**, *307*, 41.

JA0203869